Dynamical model for spin-crossover solids. II. Static and dynamic effects of light in the mean-field approach

Kamel Boukheddaden,* Isidor Shteto, Benoit Hôo, and François Varret
Laboratoire de Magnétisme et d'Optique, CNRS–Université de Versailles/St. Quentin en Yvelines, 45 Avenue des Etats Unis, F78035 Versailles Cedex, France

(Received 25 June 1999; revised manuscript received 7 August 2000)

We have introduced a photoexcitation contribution in the dynamical model we previously presented (see previous paper), as an additional term in the rate transition, in order to reproduce the light induced thermal hysteresis effect, experimentally observed in the spin-crossover materials. The set of motion equations governing the evolution of the high-spin (HS) fraction of cooperative spin-crossover systems under light, is obtained. The mean-field treatment leads to a macroscopic master equation previously given on a phenomenological basis. With both the HS→ LS (low-spin) and LS→ HS transition rates terms, a model of general use is derived. This model describes the static and dynamic properties under light. We have investigated this model analytically, as far as possible. The properties under light involve two instabilities different in nature: the high-temperature instability, chiefly entropy driven, and the low-temperature one, light induced. We have determined the conditions for these instabilities to occur, and have examined their possible collapse. The described phenomena are discussed with respect to the available data on the photoinduced bistable regime: thermal hysteresis loops, optical hysteresis loops, and transient regimes. The kinetic dependence of the photoinduced hysteresis loops is calculated.

I. INTRODUCTION

In a previous work,[1] we proposed a stochastic dynamics suitable for the spin-crossover phenomenon: an Arrhenius-type dynamical choice enabled us reproducing successfully the sigmoidal HS→LS relaxation curves experimentally observed with cooperative systems.[2] Coherently, the mean-field analysis of the proposed dynamics, established a macroscopic equation formally similar to the phenomenological one previously proposed in Ref. 3.

Recent experiments have been made on the steady state of spin-crossover systems under a permanent light,[4,5] when the thermally activated relaxation competes with the photoexcitation process. It is recalled that spin transition complexes[2] are ''thermally bistable'' systems, which undergo fluctuations (switching, crossover) between two molecular spin states, denoted LS (low-spin) and HS (high spin), and an entropy-driven spin conversion. At the solid state, under the effect of intermolecular interactions, the thermal spin-crossover may occur cooperatively; the system undergoes a first-order transition, usually associated with a thermal hysteresis, which is termed the spin transition. At low temperature, the system can be photoexcited through single-molecule processes by photons of the suited wavelength.[6] The metastable state, thus populated, has a long lifetime at low temperature. Therefore the photoexcitation process historically[6] has been termed light induced excited spin state trapping (LIESST). The LIESST phenomenon has made possible the low-temperature ($T<80$ K) investigation of the HS→LS relaxation:[3] after photoexcitation at low temperature, the sample is rapidly warmed up to the desired temperature, and relaxation is observed in the dark by magnetic measurements. High-temperature measurements of the HS↔LS relaxation are provided by Mössbauer spectroscopy, through the dynamic broadening of quadrupolar lines,[7,8] or by pulsed laser excitation.[9]

Recent experiments[4,5] have shown the possible occurrence of an instability of the steady state generated by a constant photoexcitation at moderate temperature. First, a thermal hysteresis loop has been shown by Kahn *et al.*,[4] and termed light induced thermal hysteresis (LITH). Independently, thermal and optical hysteresis loops were observed by Varret *et al.*,[5] and their cooperative origin demonstrated experimentally. The optical hysteresis loop, recorded at constant temperature as a function of the beam intensity, was accordingly termed light induced optical hysteresis (LIOH). The instability was explained by the competition between a single-molecule photoexcitation process and a cooperative thermal relaxation process. The data were well reproduced by a phenomenological macroscopic master equation,[5,10] including a linear excitation term and the nonlinear cooperative relaxation term previously proposed by Gütlich, Hauser, and Spiering[3] for explaining the sigmoidal shape of the relaxation curves of cooperative systems.

Obviously, investigating the steady states under light is but an indirect method studying relaxation. The relaxation process is merely measured through the photoexcitation process it competes with. The indirect method may provide some advantages, for example a better control of the initial state of the system, or an artificial lengthening of the lifetime of the metastable state. Also, the problems encountered for previous studies, e.g., the role of the short-range interactions[11] and the kinetics of the building-up of the correlations, will occur as well for the steady states under permanent light. In this new field of research, the occurrence of demixtion under permanent light[10] seems to be the most fascinating aspect.

The goal of the present work is to describe the dynamical

 ©2000 The American Physical Society

equations, in the general terms developed in our former work,[1] including a photoexcitation term. We present here the mean-field analysis of the model, by analytical means as far as possible, in order to outline the sensible investigations to be made under permanent light. Further developments including the effects of correlations will be presented separately.

The report is organized as follows. In Sec. II, the static and dynamic properties of the Ising-like network are briefly recalled. In Sec. III, the photoexcitation process is introduced in the master equation. In Sec. IV, the low-temperature (light-induced) instability is described and investigated analytically. In Sec. V, the coexistence of the low-temperature (light-induced) and high-temperature (entropy-driven) instabilities is examined. In Sec. VI, the kinetic effects inherent to all experimental measurements under permanent irradiation are calculated. In Sec. VII, some typical experimental data are analyzed using the present model.

II. STATIC AND DYNAMIC ANALYSIS OF THE ISING-LIKE MODEL (ADAPTED FROM REF. [1])

The phenomenological Ising-like Hamiltonian suited to describe the static properties of spin-crossover systems is written as

$$\mathcal{H}=-J\sum_{\langle i,j\rangle} s_i s_j+\sum_i \left(\Delta-\frac{kT}{2}\ln g\right)s_i, \qquad (2.1)$$

where $J>0$ is the intermolecular ''ferromagneticlike'' coupling between spin-crossover molecules, and s the fictitious spin with eigenvalues $+1$, -1 associated with the two spin states HS, LS, respectively. Δ is the ligand field splitting, i.e., the energy difference $E(\mathrm{HS})-E(\mathrm{LS})$ of isolated molecules, g the degeneracy ratio between the HS and LS states, and k the Boltzmann constant.

As it has been shown in Ref. 1, in the mean-field approximation, this model has an analytical solution and leads to a thermal first-order transition if the thermodynamical equilibrium temperature $T_{\mathrm{eq}}=2\Delta/\ln g$ is smaller than the order-disorder temperature $T_C=qJ$, with q the coordination number of the spin-crossover units. For further details on the static analysis of the Ising-like Hamiltonian, the reader should refer to the pioneering paper of Wajnsflasz and Pick.[12,13]

The dynamics of the model, introduced in Ref. 1 following the stochastic approach of Glauber[14,15] was studied with an appropriate Arrhenius-like dynamics, and led us to obtain, in the mean-field approach,[16] the following evolution equation on the high spin fraction n_{HS}:

$$\frac{dn_{\mathrm{HS}}}{dt}=\frac{2}{\tau_0}[(1-n_{\mathrm{HS}})e^{-\beta\Delta E_{\mathrm{LH}}}e^{2\beta qJn_{\mathrm{HS}}} - n_{\mathrm{HS}}e^{-\beta\Delta E_{\mathrm{HL}}}e^{-2\beta qJn_{\mathrm{HS}}}], \qquad (2.2)$$

where E_a^0 is the intramolecular energy barrier corresponding to the saddle point energy in the configurational diagram[2] of the system, ΔE_{LH} and ΔE_{HL} are effective barriers (including the intramolecular one) between LS and HS states, and τ_0 is a scale time factor. They are given by

$$\Delta E_{LH}=-E_a^{(0)}-\Delta-qJ+\frac{kT}{2}\ln(g),$$

$$\Delta E_{HL}=E_a^{(0)}-\Delta-qJ+\frac{kT}{2}\ln(g). \qquad (2.3)$$

We recall that Eq. (2.2), reproduces exactly at low temperature the empirical equation proposed by Hauser *et al.*[17,18] describing the sigmoidal shape of the experimental relaxation curves of the high spin fraction after photoexcitation.

III. PHOTOEXCITATION

The photoexcitation of spin-crossover systems was shown by pulsed laser experiments[9] and popularized by the low-temperature direct and reverse processes, termed light induced excited spin state trapping (LIESST).[19] It is based on a Franck-Condon optical absorption (metallic *d-d* band or metal-to-ligand charge transfer band), followed by a radiationless nonadiabatic relaxation toward the excited (metastable) spin state. The features of this nonadiabatic relaxation are central with respect to the properties of the photoexcited system.

Historically, these problems have been addressed first in the fields of photochemical reactions of solids[20] and light-induced ordering of alloys.[21] Recently, cooperative photoexcitation processes, termed the DOMINO effect, have been evidenced at the neutral-to-ionic transition,[22–24] and their modelization, accounting for the lattice dynamics, is being worked out.[25,26]

As for the spin-crossover systems, for a long time there was no evidence for a cooperative character of the photoexcitation process in itself. But, recent experiments under pulsed laser excitation[27] have given a first one of the onset of cooperative photoexcitation.

Here we do not aim at addressing a general problem accounting for the interaction between the structural distortions and the photoexcitation process. Alternatively, we propose, for the effect of light, a phenomenological approach of the photoexcitation process, neglecting the photoinduced local stresses and distortions.

The rigorous resolution of the photoexcitation phenomenon would require the knowledge of the total Hamiltonian, including the electromagnetic field, based on the actual interactions of light with matter. Since the interactions are not precisely known in the present case, and for putting the model in the most general terms, we propose a phenomenological dynamics under irradiation just based on the Ising-like model, in the same way to the competing dynamics between Glauber spin-flip and spin-exchange Kawasaki processes, studied in the literature.[28] Therefore, the proposed rate transition expression is obtained by a modification of the HS$\leftrightarrow$LS transition probabilities.

The total rate transition for the jth spin to flip from s_j to $-s_j$ is written as the sum of two transition probabilities associated with two events, of thermal and of optical origin. The mutually excluding character of these events, and the stochastic treatment given to the total transition probability are based on some assumptions which need to be developed, as follows.

First of all, the main assumption lies in the absence of

coupling between the thermal and optical processes. This requires the photon flux should not sizably warm up the system. Second, the effect of stimulated transitions is disregarded here. Also, the time scales of the thermal and optical processes are very different,[29,30] since the thermal fluctuations are assumed to follow adiabatically the photon flux (quasicontinuous flux). The latter assumption compares to the Born-Oppenheimer approximation which ''decouples'' the (slow) motions of the nuclei and the (fast) motions of the electrons. In other words, the photoexcitation process is considered as instantaneous, with respect to the thermodynamical relaxation times. If this was not the case, the adiabatic and Markovian character of the process would be lost.

We restrict here the description to the LS→HS optical process, corresponding to the monochromatic irradiation of spin-crossover solids with green light (of course, accounting for both the direct and reverse = red light optical processes should be straightforward). Within the choice of the dynamics already explicit,[1] the total (thermal + optical) transition probability is written

$$W(s_j)=\frac{1}{2\tau}[(\cosh\beta E_j - s_j \sinh\beta E_j)]+\frac{I_0\sigma}{2}(1-s_j), \tag{3.1}$$

with $E_j=-J\Sigma_i s_i+[\Delta-(kT/2)\ln g]$ and $1/\tau=(1/\tau_0)e^{-\beta E_a^{(0)}}$. I_0 is the intensity of the incident irradiation, σ the absorption cross section, based on the actual quantum mechanical data of the photoexcitation process,

The temporal evolution of the average $\langle s_j\rangle$, obtained through the master equation[1] and the transition rate [Eq. (3.1)], writes $d\langle s_j\rangle/dt=-2\langle s_j W(s_j)\rangle$; which gives

$$\frac{d\langle s_j\rangle}{dt}=I_0\sigma(1-\langle s_j\rangle)+\frac{1}{\tau}(-\langle s_j\cosh\beta E_j\rangle+\langle\sinh\beta E_j\rangle). \tag{3.2}$$

In the mean-field approximation previously defined, and assuming the spatial invariance of the lattice, the evolution equation is expressed in terms of the HS fraction n_{HS} $(=1+\langle s\rangle/2)$, as follows:

$$\frac{dn_{HS}}{dt}=2I_0\sigma(1-n_{\mathrm{HS}})+\frac{2}{\tau_0}(1-n_{\mathrm{HS}})e^{\beta\Delta E_{LH}}e^{2\beta qJn_{\mathrm{HS}}} - \frac{2}{\tau_0}n_{\mathrm{HS}}e^{-\beta\Delta E_{HL}}e^{-2\beta qJn_{\mathrm{HS}}}. \tag{3.3}$$

This is exactly, completed by the LS→HS relaxation term, the phenomenological equation already used in Ref. 5.

Remarks. (i) *On the optical process.* The optical probability has been written here as a single-site process, i.e., the possible cooperative aspects, such as the ''domino effect,''[25] have been disregarded. To account for cooperative effects, we must introduce the lattice relaxation associated with the local excitation. In this case, the global structural change occurs only when the intersite interaction is short-ranged and moderately strong.[23] In our problem, the cross section should be written as a function of the microscopic configuration $(s_1,s_2,\ldots,s_i,\ldots,s_N)$ of the system and the state of the lattice.

(ii) *On the choice of the correct dynamics.* In addition to the present Arrhenius-like dynamics, we have considered the genuine Glauber dynamics and the time-dependent Ginzburg-Landau (TDGL) dynamics. The Glauber dynamic leads to transition probabilities and mean-field motion equations which apparently little differ from the present Arrhenius-like dynamics

$$W_1^G(s_j)=\frac{1}{2\tau}(1-s_j\tanh\beta E_j)+\frac{I_0\sigma}{2}(1-s_j) \tag{3.4}$$

and

$$\left(\frac{dm}{dt}\right)^G=\frac{1}{\tau}\left(-m+\tanh\beta\left[qJm-\Delta+\frac{kT}{2}\ln g\right)\right] + I_0\sigma(1-m). \tag{3.5}$$

The TDGL dynamics is a macroscopic dynamics suited to systems the free energy of which $F(m)$ has a double-well dependence with respect to the order parameter. The motion equation is written as

$$\left(\frac{dm}{dt}\right)^{\mathrm{TDGL}}=-\frac{A}{2\tau}\frac{\delta F}{\delta m}+\frac{I_0\sigma}{2}(1-m). \tag{3.6}$$

Accounting for the free-energy expression of the Ising-like system

$$F(m)=\frac{1}{2}qJm^2-kT\ln\left\{2g\cosh\beta\left(qJm-\Delta+\frac{kT}{2}\ln g\right)\right\}. \tag{3.7}$$

The motion equation is written

$$\left(\frac{dm}{dt}\right)^{\mathrm{TDGL}}=+\frac{AqJ}{\tau}\left[-m+\tanh\beta\left(qJm-\Delta+\frac{kT}{2}\ln g\right)\right] + I_0\sigma(1-m). \tag{3.8}$$

Unfortunately, the low-temperature behavior generated by Eqs. (3.5) and (3.8) does not yield the light-induced bistability. Accordingly, both of the Glauber and TDGL dynamics did not yield the self-accelerated character of the relaxation in the dark.[1] The same work was also made with the Metropolis dynamics and led to the same conclusion.

(iii) It is worth quoting a previous work,[31] using Monte Carlo simulations, aiming to explain the photoinduced behavior of Fe-Co Prussian blue analog: this is a diamagnetic in the dark, and turns to a ferrimagnet after illumination.[32,33] The intuitous analogy between spin-crossover solids and this Prussian blue analog (both are photoexcitable solids) was recently ascertained by the observation of cooperative relaxation (sigmoidal time dependence) of the photoexcited state in the latter compound.[34] Therefore a common approach should apply, and the basic assumption of Ref. 31, treating the effect of the light as a renormalization of the magnetic anisotropy and temperature, reveals to be unappropriate: it indeed leads to a simple light induced shift of the phase diagram, at variance from the complex behavior exhibited by the spin crossover solids (and analyzed in the present work).

IV. THE LOW-TEMPERATURE REGIME AND THE LIGHT-INDUCED INSTABILITY

It is known now[4,5] that under continuous irradiation, the steady states of the spin-crossover system may exhibit hysteresis loops, either thermal (= LITH, at constant intensity), or optical (= LIOH, at constant temperature). These hysteretic effects will be described here by analytical means, in a mean-field approach, i.e., in absence of correlations and thermal fluctuations. Future work will be devoted to further approaches.

We start with the study of the steady states (dynamic equilibrium) of the system at low temperature, for which the thermal LS↦HS relaxation is hindered by a large energy barrier [refer to the expression given for ΔE_{LH} in Eq. (2.3)]. The general situation for which both relaxation processes are efficient will be analyzed in Sec. V, and time-dependent effects will be analyzed in Sec. VI.

The low-temperature evolution equation is written

$$\frac{dn_{\mathrm{HS}}}{dt}=2I_0\sigma(1-n_{\mathrm{HS}})-\frac{2}{\tau_0}n_{\mathrm{HS}}e^{-\beta\Delta E_{HL}}e^{-2\beta qJn_{\mathrm{HS}}}. \tag{4.1}$$

This equation, already given in Ref. 5 might describe, as well, a chemical reaction far from equilibrium. Indeed chemical reactions may exhibit spectacular features, such as spacial patterns in shape of rings, spirals, which spontaneously develop in an initially homogeneous medium, associated with transient compositional fluctuations,[35] turbulent regimes. Such fascinating features originate from the nonlinear characters of the evolution equations.

A. The dynamic potential

The concept of dynamical potential, related with the Lyapunov function, at one variable (n_{HS} here) has been introduced by Tomita *et al.*[36] for studying the relaxation of the metastable states of an Ising system. We use it here for visualizing the stability properties of the steady states under permanent irradiation. The principle is the following: the flux dn_{HS}/dt expressed by the evolution equation, is considered as proportional to a driving force which is the derivative of a dynamic potential denoted U. This actually corresponds to the 1D motion of a material point with viscous friction and negligible inertia, in the potential U. The motion equation is written:

$$\frac{dn_{\mathrm{HS}}}{dt}=-\frac{\partial U}{\partial n_{\mathrm{HS}}}. \tag{4.2}$$

Accordingly, we calculate the dynamic potential associated with the expression of the flux [Eq. (4.1)], as

$$U(n_{\mathrm{HS}},T,I_0)=-2I_0\sigma\left(n_{\mathrm{HS}}-\frac{n_{\mathrm{HS}}^2}{2}\right)-\frac{1}{\beta qJ}e^{-2\beta qJn_{\mathrm{HS}}} \times\left(n_{\mathrm{HS}}+\frac{1}{2\beta qJ}\right)\frac{e^{-\beta\Delta E_{HL}}}{\tau_0}. \tag{4.3}$$

We show in Fig. 1 a double-well potential, typical for a bistable situation, calculated for suited values of the model parameters ($T=70$ K, $\sigma I_0\tau_0=1\times510^{-4}$).

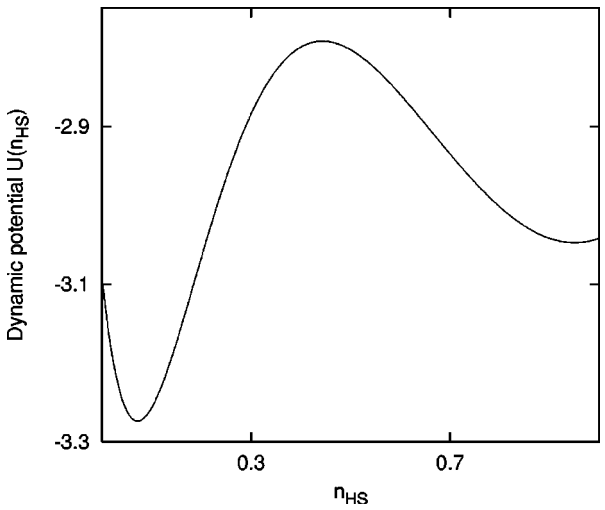

FIG. 1. The dynamic potential associated with a bistable situation of the system under permanent irradiation. Parameter value are $qJ=220$ K, $\Delta=500$ K, $g=150$, $I_0\sigma\tau_0=3\times10^{-5}$, $E_a^{(0)}=900$ K, and $T=70$ K. The steady states of the system correspond to the two minima of the curve.

We illustrate the bistable character associated with the double-well dynamic potential shown above, by the time dependence curves of the system. As shown in Fig. 2, the evolution of the system is governed by the initial state, i.e., bistability occurs as a ''memory effect'' in the system. Of course, bistability, hysteresis and memory effects are tightly related altogether.

Analytically, the steady states shown in Fig. 2 can be derived by setting $dn_{\mathrm{HS}}/dt=0$, i.e., $\partial U/\partial n_{\mathrm{HS}}=0$ (the dynamic potential is minimized), which leads to the state equation of the steady states $n_{\mathrm{HS}}(T,I)$.

$$I_0\sigma(1-n_{\mathrm{HS}})=\frac{1}{\tau_0}n_{\mathrm{HS}}e^{-\beta\Delta E_{HL}}e^{-2\beta qJn_{\mathrm{HS}}}. \tag{4.4}$$

The numerical resolution of the n_{HS}-self-consistent equation can be avoided, by expressing T as a function of n_{HS} and I. The optical hysteresis loop is obtained straightforwardly as a function of n_{HS}. The behavior of the steady states is now analyzed in detail in the coming sections.

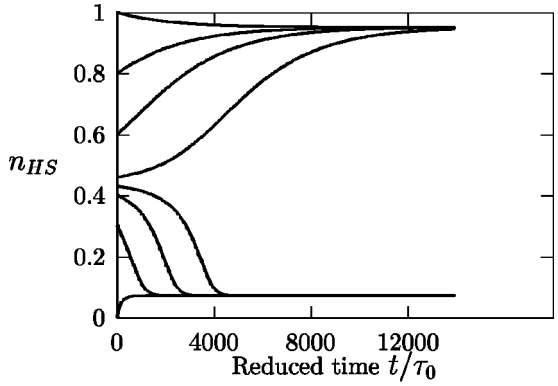

FIG. 2. Time dependence of the high-spin fraction in the case of light-induced bistability conditions. The different curves result from different initial conditions. Parameter values are those of Fig. 1.

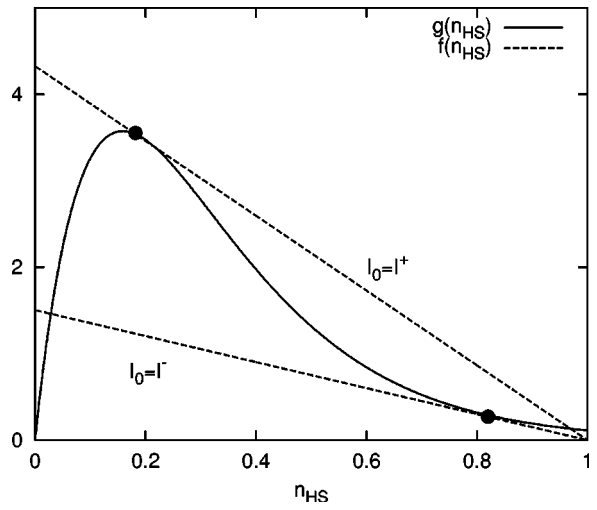

FIG. 3. The graphical resolution of the state equation of the steady states Eq. (4.6), for the same parameters as Figs. 1,2 (except for I_0). $f(n_{\mathrm{HS}})$ is the photoexcitation term, straight line, and $g(n_{\mathrm{HS}})$ is the relaxation term. The two limiting situations ($I_0=I^+,I^-$) have been presented.

B. The low-temperature bistability condition

The occurrence of low-temperature bistability is derived from a simple graphical approach (adapted from Ref. 5). The steady states [Eq. (4.4)] can be obtained by intersecting the following functions

$$f(n_{\mathrm{HS}})=2I_0\sigma(1-n_{\mathrm{HS}}),$$

$$g(n_{\mathrm{HS}})=\frac{2}{\tau_0}n_{\mathrm{HS}}e^{-\beta\Delta E_{HL}}e^{-2\beta qJn_{\mathrm{HS}}}. \tag{4.5}$$

$f(n_{\mathrm{HS}})$ is a straight line with a slope proportional to the applied intensity I_0. On the contrary, $g(n_{\mathrm{HS}})$ has a strong nonlinear character, temperature dependent, with an inflexion point at $n_{\mathrm{HS}}=1/(\beta qJ)$.

The bistable situation is shown in Fig. 3. At constant temperature, the intensity is varied, i.e., the slope of straight line is changed, and the number of solutions may be either one (monostable situation) or three (bistable situation). In the latter case, two solutions are stable, separated by an unstable solution. There are, on varying intensity, bifurcations between the monostable and bistable situations. These bifurcations are denoted here ''spinodes'' and the term strictly refers to the steady states, at variance from a previous report dealing with ''transient'' instabilities.[10]

The spinodes here define the limits of the bistable regimes, i.e., of the hysteresis loops, and therefore will be investigated thoroughly. At the spinodes, the functions $f(n_{\mathrm{HS}})$, $g(n_{\mathrm{HS}})$ are equal and have equal derivatives, such that

$$2I_0\sigma(1-n_{\mathrm{HS}})=\frac{2}{\tau_0}n_{\mathrm{HS}}e^{-\beta\Delta E_{HL}}e^{-2\beta qJn_{\mathrm{HS}}},$$

$$-2I_0\sigma=\frac{2}{\tau_0}e^{-\beta\Delta E_{HL}}e^{-2\beta qJn_{\mathrm{HS}}}(1-2\beta qJn_{\mathrm{HS}}). \tag{4.6}$$

This set of equations is solved by expressing $e^{-2\beta qJn_{\mathrm{HS}}}$ in the second one, and then substituting it in the first one. The n_{HS} second degree equation is obtained:

$$(1-n_{\mathrm{HS}})(1-\alpha n_{\mathrm{HS}})+n_{\mathrm{HS}}=0, \tag{4.7}$$

where

$$\alpha=2\beta qJ. \tag{4.8}$$

Such an equation has acceptable solutions for $\alpha>4$ only. This is the Prigogine condition, previously expressed for the similar nonlinear equation associated with the cooperative adsorption-desorption process of molecules on a surface.[37]

1. Light-induced equilibrium temperature

The state equation (4.4) of the steady states enables expressing temperature as a function of the other variables as

$$\beta=\frac{1}{\Delta+qJ-E_a^{(0)}-2qJn_{\mathrm{HS}}}\ln\left(I_0\sigma\tau_0\sqrt{g}\,\frac{(1-n_{\mathrm{HS}})}{n_{\mathrm{HS}}}\right). \tag{4.9}$$

A light-induced equilibrium temperature is obtained by setting $n_{\mathrm{HS}}=1/2$ in the previous equation. It turns out that

$$T_{1/2}=\frac{T_{\mathrm{eq}}-T^{(0)}}{1+\ln\sigma I_0\tau_0/\sqrt{g}}, \tag{4.10}$$

with $T^{(0)}=2E_a^{(0)}/k_B\ln(g)$.

The light-induced temperature depends the degeneracy ratio g and on the dimensionless intensity parameter $\tau_0\sigma I_0$. It does not depend on the interaction parameter J, just as in the ''static'' (i.e., entropy-induced) equilibrium temperature $T_{\mathrm{eq}}=2\Delta/k_B\ln(g)$.

According to the above expressions of the static and of the light induced equilibrium temperatures, it is suggested that the effect of light on the steady states is equivalent to renormalizing the degeneracies and the ligand-field. This can be put in terms of a competition between ''effective'' degeneracies, static and dynamic.

2. Light-induced thermal hysteresis (LITH) loops

The existence of thermal hysteresis loops is a direct consequence of the bistability presented in the previous section. The bistability condition $\alpha>4$ can be expressed in temperature terms $T<T_C^*=qJ/2k_B$. Above T_C^*, the system has a single steady state, it is ''monostable.'' Typical bistable behaviors below T_c are illustrated by the dynamic potential curve in Fig. 1 and by the set of $n_{\mathrm{HS}}(T)$ curves, computed for several I_0 values, shown in Fig. 4.

The behavior analogy with that of the first-order van der Waals theory has been outlined.[38] However, this analogy should not extend until the metastable states properties, since this concept does not apply to the present case of an open thermodynamic system (submitted to a permanent energy flux).

The spinodal curve is the locus of the instability points in the parameter space (T,I_0,n_{HS}). These instability points have been shown in Fig. 3, corresponding to the limiting values of the slope of the straight line. Accordingly, in our

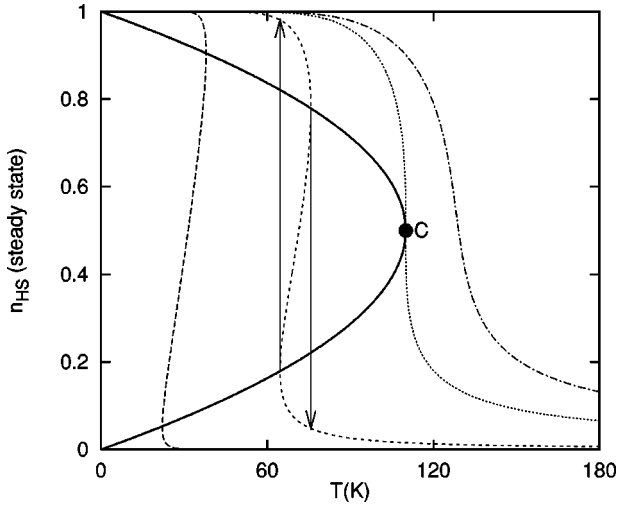

FIG. 4. Light-induced steady states and thermal hysteresis (LITH) loops, with the corresponding light-induced thermal spinodal curve (thick full line). The parameter values which are those of Figs. 1–3 excepted intensity values are $I_0\sigma\tau_0(\times 10^5)=0.005,15,136.5=I_0^C\sigma\tau_0=(1/\sqrt{g})e^{-2(E_a^0-\Delta)/qJ}$ (critical value), and 250.

previous paper,[10] this locus had been denoted the ''limiting curve of the hysteresis loops in the phase diagram.'' Here we calculate it according to the properties of the dynamic potential, at the limit situation where the stable state is also an inflexion point. The equations to be combined are: $\partial^2 U/\partial n_{\rm HS}^2=0$ (spinodes) and $\partial U/\partial n_{\rm HS}=0$ (state equation). Each of these equations define a surface in the parameter space $(T,I_0,n_{\rm HS})$, their intersection is the spinodal curve. Since it is associated with the light-induced steady states, this curve will be denoted the light-induced spinodal curve. The projections along the $(T,n_{\rm HS})$, and $(I_0,n_{\rm HS})$ planes will be denoted the thermal light-induced spinodal curve and the optical light-induced spinodal curve. The projection along the (T,I_0) plane is the phase diagram of the system.

Alternatively, the thermal or optical light spinodal curves can be obtained by combining the state equation of the steady states and the conditions for infinite (or null) slopes: $\partial I_0/\partial n_{\rm HS}=0$ and $\partial T/\partial n_{\rm HS}=0$. Setting to zero the second derivative of the dynamical potential yields

$$n_{\rm HS}=\frac{1}{2}\left(1\pm\sqrt{1-\frac{4}{\alpha}}\right). \tag{4.11}$$

By substituting $\alpha=2\beta qJ$, the light-induced thermal spinodal is derived:

$$\frac{kT}{2}=qJn_{\rm HS}(1-n_{\rm HS}). \tag{4.12}$$

It is plotted in Fig. 4, together with the thermal curves associated with the dynamic equilibrium. Both of them are drawn in the $n_{\rm HS}$-T plane. The thermal light-induced spinodal curve is reminiscent of the spinodal curve of the equilibrium state, determined in Ref. 1. However, the latter is generated by varying the electronic gap parameter, while the former by varying the applied intensity, and the critical temperatures differ by a factor of 2, with $T_C=qJ/k_B$ for the static equilibrium and $T_C^*=qJ/2k_B$ for the steady states under permanent light.

There is a critical value for the intensity, above which the thermal hysteresis no longer occurs:

$$\sigma I_C^*=\frac{1}{\tau_0\sqrt{g}}\,e^{-2[(E_a^0-\Delta)/qJ]}. \tag{4.13}$$

At the critical intensity value, $n_{\rm HS}=1/2$ and $T=T_C^*=qJ/2k_B$. This indeed defines the light-induced critical point in the parameter space.

3. Light-induced optical hysteresis (LIOH) loops

The optical curves, at constant temperature, are given by the state equation, expressed as:

$$\sigma I_0=\frac{1}{\tau_0}\,\frac{n_{HS}}{1-n_{HS}}\,e^{-\beta\Delta E_{HL}}e^{-2\beta qJn_{HS}}. \tag{4.14}$$

In analogy with the previously defined equilibrium temperature, an equilibrium intensity $\sigma I_{1/2}$, is defined so that it yields $n_{\rm HS}=1/2$. Substituting in the previous equation,

$$\sigma I_{1/2}=\frac{1/\tau_0}{\sqrt{g}}\,e^{-\beta(E_a^{(0)}-\Delta)}. \tag{4.15}$$

The equilibrium intensity $\sigma I_{1/2}$, as the equilibrium temperature, does not depend on J. It depends on temperature, and increases for increasing temperature; at the high-temperature limit, $\sigma I_{1/2}$ tends to the finite value

$$\sigma I_{1/2}(T_\infty)=\frac{1}{\tau_0\sqrt{g}}. \tag{4.16}$$

A set of computed optical curves , with the light-induced optical spinodal curve, is shown in Fig. 5. The lower and upper values of the optical hysteresis loop are easily expressed as

$$\sigma I_0^{\pm}=\frac{1}{\tau_0}\left(1\mp\sqrt{1-\frac{4}{\alpha}}\right)e^{-\beta\Delta E_{HL}}e^{-(\alpha/2)(1\pm\sqrt{1-(4/\alpha)})} \tag{4.17}$$

These expressions illustrate the intensity threshold effect previously reported[5]: the larger the coupling constant J, the stronger the threshold effect.

The light-induced optical spinodal curve is obtained by eliminating temperature between the state equation and $\partial^2 U/\partial n_{\rm HS}^2=0$. It is

$$\sigma I_0=\frac{1}{\tau_0\sqrt{g}}\,\frac{n_{\rm HS}}{1-n_{\rm HS}}\,e^{-1/(1-n_{\rm HS})}e^{-(\Delta+E_a^{(0)}-qJ)/2qJn_{\rm HS}(1-n_{\rm HS})}. \tag{4.18}$$

4. Phase diagram

The phase diagram in $(T-I_0)$ axes can be obtained by eliminating $n_{\rm HS}$ between the state equation and $\partial^2 U/\partial n_{\rm HS}^2=0$; alternatively, by plotting $\omega I_0^{\pm}$ as a function of T (for

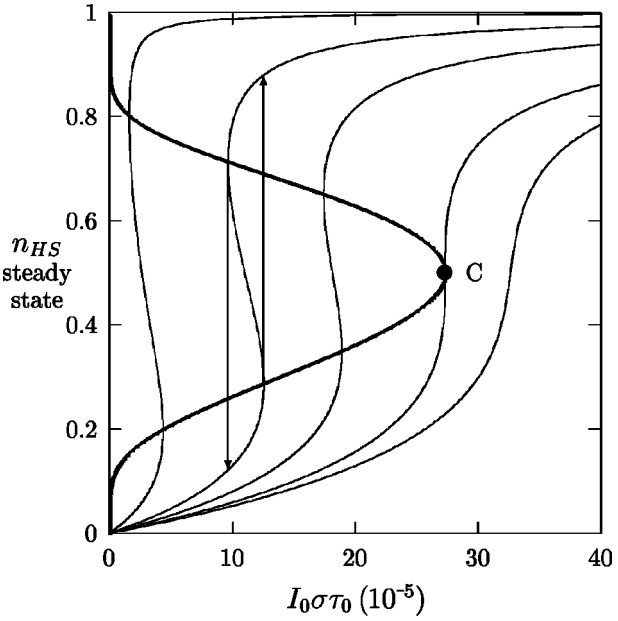

FIG. 5. Light-induced steady states and optical hysteresis (LIOH) loops, with the corresponding light-induced optical spinodal curve (thick full line). Parameter values are those of Figs. 1,2, excepted for $T=70$, 90, 100, 110 K$=T_C=qJ/2k_B$ (critical value), and 115 K from left to right.

given Δ,J,g). It is shown in Fig. 6; in-between the dotted curves is the diphasic region, which ends at the critical point.

5. Light-induced pressure hysteresis (LIPH) loops

Application of pressure to spin-crossover solids usually favors the low-spin state because it has the smaller volume. In the Ising-like model the effect of pressure p is easily accounted for by a change in the electronic (enthalpic) gap Δ

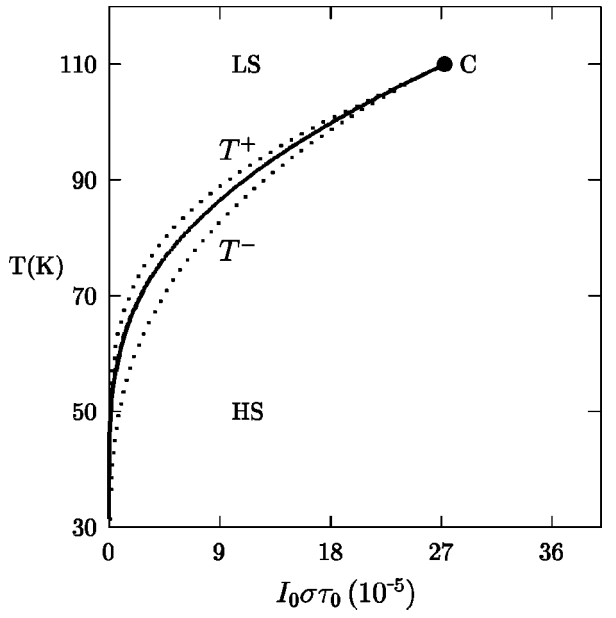

FIG. 6. The phase diagram of the light-induced steady states in the $I_0\sigma\tau_0,T$ plane, with the equilibrium line represented as a full line $[I_{1/2}(T)\Leftrightarrow T_{1/2}(I_0)]$. In between T^+,T^- is the hysteretic region. Parameter values as those of Figs. 1,2 (except for I_0, T).

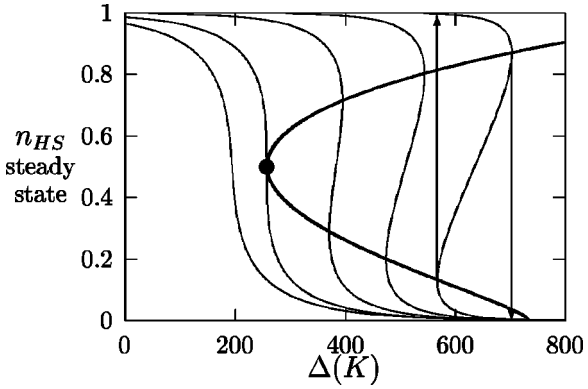

FIG. 7. Light-induced steady states and pressure hysteresis (LIPH) loops, with the corresponding light-induced pressure spinodal loop (at constant intensity). Parameter values are those of Figs. 1,2, except for the Δ variable and $T=120$, $110=T_C=qJ/2k_B$ (critical value) and 90, 70, and 50 K from left to right.

$=\Delta_0+p\Delta V$, where ΔV is the difference in molecular volume $\Delta V=V(\mathrm{HS})-V(\mathrm{LS})>0$. Since ΔV is system dependent, we shall rather investigate the role of pressure through the variable Δ, in the equations developed so far.

As seen in the previous sections, the low-temperature light-induced instability is responsible for hysteresis loops as a function of T, I. It will also result in hysteresis loops as a function of p. Accordingly, the latter effect will be denoted light-induced pressure hysteresis (LIPH) loops. Such LIPH loops, computed for different temperature values, but equal intensities, are reported in Fig. 7.

The state equation (4.4) of the steady states is conveniently reexpressed as

$$\Delta=E_a^0+qJ(2n_{\mathrm{HS}}-1)+kT\ln\left(I_0\sigma\tau_0\sqrt{g}\,\frac{1-n_{\mathrm{HS}}}{n_{\mathrm{HS}}}\right). \tag{4.19}$$

A transition pressure $p_{1/2}$ (corresponding to $\Delta_{1/2}$) can be defined as the pressure (enthalpic gap or ligand-field value) leading to the equipopulation of the two levels. It is derived from Eq. (4.19) by setting $n_{\mathrm{HS}}=1/2$. It is

$$\Delta_{1/2}=E_a^0+kT\ln(I_0\sigma\tau_0\sqrt{g}). \tag{4.20}$$

As for $T_{1/2}$ and $I_{1/2}$, the equilibrium pressure $p_{1/2}$ does not explicitly depend upon the interaction parameter J; the reason is obvious in the mean-field approximation used. On the contrary, $p_{1/2}$ depends tightly on the barrier energy E_a^0, according to the explicit dependence given in Eq. (4.20). It is also worth remarking the linear dependence of $p_{1/2}$ with respect to temperature. Such a particular dependence makes very attractive the comparison with experimental data, which are expected in the next future.[39]

The limit pressure values, i.e., the edges of the LIPH loops, represented here by $\Delta^{\pm}$, are derived from the relation $\partial\Delta/\partial n_{\mathrm{HS}}=0$. They are rather obtained through the corresponding steady-state n_{HS} values

$$n_{\mathrm{HS}}^{\pm}=\frac{1\pm\sqrt{1-2kT/qJ}}{2}. \tag{4.21}$$

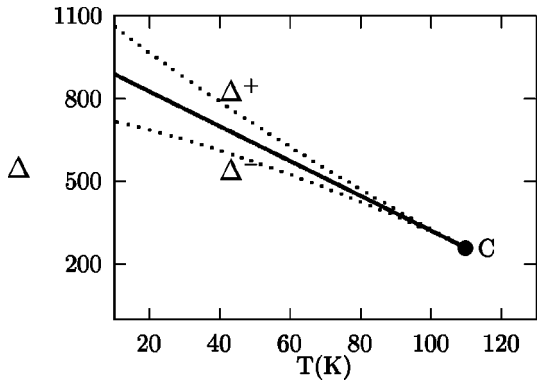

FIG. 8. The phase diagram of the light-induced steady states in the Δ, T plane (pressure effect). Parameter values are those of Figs. 1,2 (except for Δ, T). In between Δ^+, Δ^- is the hysteretic region. The straight line stands for the equilibrium pressure ($\Delta_{1/2}$).

The light-induced spinodal curve, projected on the $(\Delta, n_{\mathrm{HS}})$, i.e., the light-induced pressure spinodal curve, is then given by

$$\Delta = 2qJn_{\mathrm{HS}}(1-n_{\mathrm{HS}})\ln\left\{\sqrt{g}\frac{I_0\sigma}{1/\tau_0}\frac{kT}{2qJn_{\mathrm{HS}}^2}\right\} + E_a^0 + qJ(2n_{\mathrm{HS}}-1). \tag{4.22}$$

The critical value Δ_C^*, below which the system will not exhibit the light-induced instability, is derived from Eq. (4.22) with $n_{\mathrm{HS}}=1/2$ and $T_C^*=qJ/2k_B$. It is

$$\Delta_C^* = E_a^0 + \frac{qJ}{2}\ln\sqrt{g}I_0\sigma\tau_0. \tag{4.23}$$

The LIPH loops calculated for several temperature values (see Fig. 7) show that the lower the temperature, the larger the width of the pressure loop. From the practical viewpoint, experiments will be easier, i.e., the observation of LIPH loops will require lower pressures, near the critical point. A typical pressure-temperature phase diagram (for given J, g, $\tau_0 I_0 \sigma$ values) is reported in Fig. 8.

V. ENTROPY-DRIVEN AND PHOTO-INDUCED BISTABILITIES

In this section, we deal with higher temperatures such that both the HS-LS and LS-HS relaxations have to be accounted for, according to the complete macroscopic master equation (3.3). In other words, we consider in the same model both the low-temperature light-induced bistability, previously described, and the high-temperature, entropy-driven bistability, i.e., the usual static spin transition. We have resolved this equation numerically, by continuity, in order to describe the thermal behavior of the steady states. This corresponds to the experimental situation of a system under permanent irradiation, submitted to an ideally slow temperature sweep. The calculated curves of the high-spin fraction are reported in Fig. 9.

It clearly appears that increasing intensity will tend to raise the temperature of the light-induced loop, and to lower that of the entropy-driven loop. A collapse of the two loops

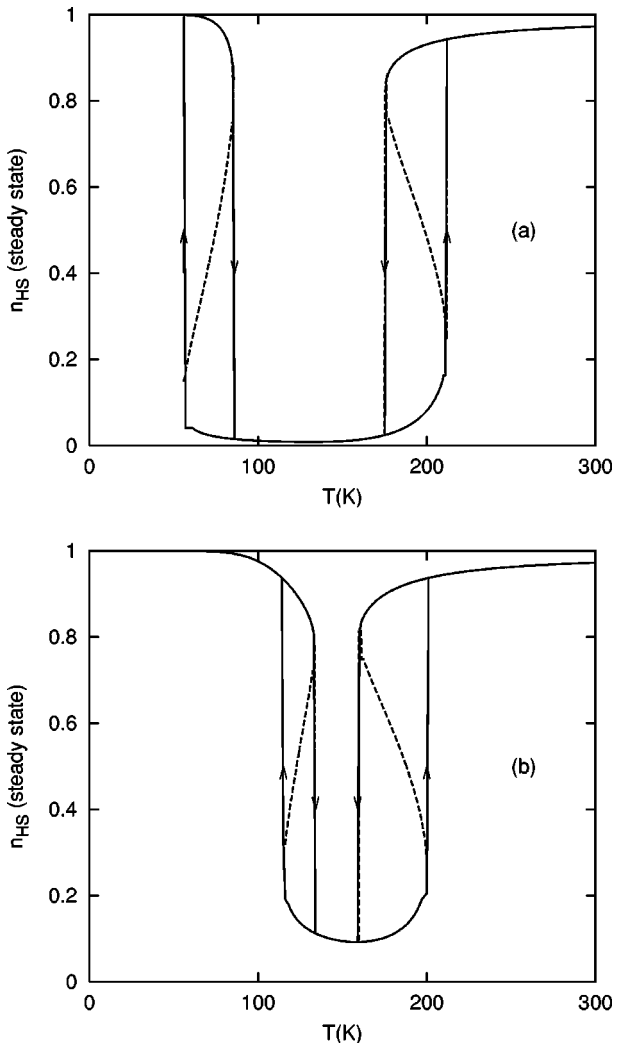

FIG. 9. The double instability of the light-induced steady states: the low-temperature, chiefly light-induced, and the high-temperature, chiefly entropy driven, for different I_0 values. Parameter values are $qJ=300$ K, $\Delta=500$ K, $g=150$, $I_0\sigma\tau_0(\times 10^5)=5$ (a), 50 (b).

can be expected for a threshold value of intensity, such that the upper value T^+ of the light-induced loop and the lower value T^- of the entropy-driven loop have joined each other. Above this threshold value, the curve of the steady state will split in two parts, as shown in Fig. 10. In such a situation, the complex behavior of the system is described as follows: starting from any of the extreme temperatures, the system will continuously follow the upper line and will not visit the states belong to the isolated, droplet-shaped part of the curve. However, it can be forced to visit these states by a transient variation of the other parameters (e.g., intensity). For example, the system can be prepared at 150 K, in the dark. Initially, it is in the LS state (see A in the figure). By switching on the light, the system will reach a steady state of prominent LS character (see B). This is a metastable state, since for a sufficient increase (C,D) or decrease (E,F) in temperature, the system will irreversibly switch to the prominently HS steady state. In other words, the system describes open hysteresis loops.

The complete experimental investigation of such an effect is a fascinating game which requires, at the present state of

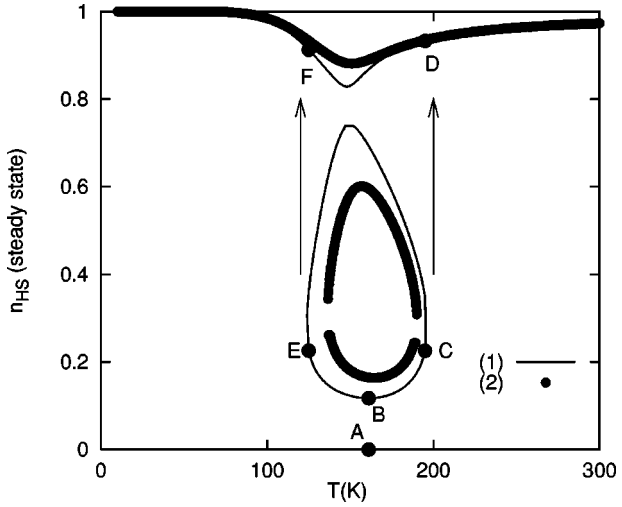

FIG. 10. The collapse of the instability loops, following Fig. 10, with larger intensity values: $I_0\sigma\tau_0(\times 10^5)=60$ (1, thin line), 75 (2, thick line). The bottom parts of the curves are metastable, the top ones are stable.

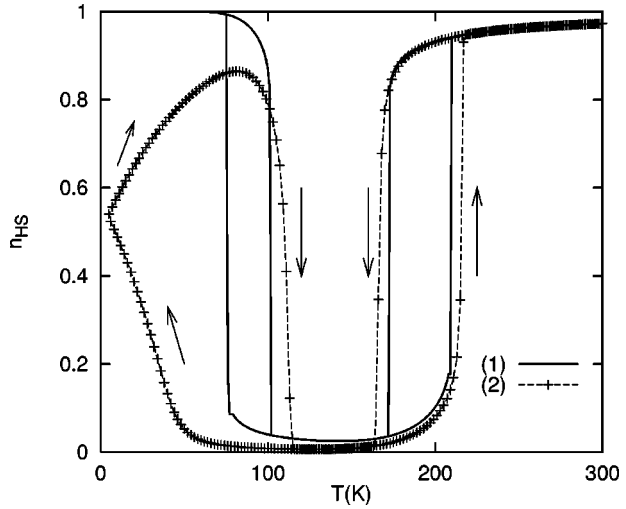

FIG. 11. A typical kinetic distortion of the thermal hysteresis loops (crosses=2) with respect to the dynamic equilibrium curve (steady states, full line=1). The temperature sweep rate $\tau_0 dT/dt = 8.10^{-3}$ K. The parameter values are those of Fig. 10, with $I_0\sigma\tau_0(\times 10^5)=1.5$.

art, a large improvement in the yields of photoexcitation, or the use of high-power sources of light. The discovery of new complexes with longer relaxation rates would provide additional experimental opportunities for these peculiar, reentrantlike, memory effects.

VI. KINETIC EFFECTS ON THE HYSTERESIS LOOPS

Experiments aiming to observe the light-induced steady states and the various hysteresis loops involve kinetic parameters, due to the finite time available for the measurements. The steady states are only approximatively reached, and hysteresis loops are expected to be distorted (enlarged) by kinetic contributions.

Schematically, the kinetic effects can arise from two ways: (i) the finite (nonzero) sweep rate dx/dt of the variable parameter $x=T,I_0,p$, along which the hysteresis loop $x-n_{\mathrm{HS}}$ is measured, (ii) the waiting time, i.e., the preparation time of a system before the measurements, for example, as a function of time, are started. In more general terms, the thermopiezo-optical history of the system has to be accounted for.

We mainly investigate here the kinetic aspects related to the sweep rate. The available experimental data,[5] recorded at rather low temperatures (<70 K), give evidence of such kinetic effects, in spite of the long measurement time (days for a LITH or LIOH loop). It is noteworthy that the kinetic effects are enhanced in the bulk of the sample, due to absorption of light, so that reflectivity data which are associated with the surface properties of the sample,[40] should be preferred.

Calculations accounting for the kinetic effects require resolving the evolution equation (3.3) of the system, completed by the time dependence of the considered variable, through a kinetic equation such as $x=f(t)$, where $x=T,I_0,p$. The resolution of the set of coupled equations has to be made numerically. We have performed such numerical resolutions, with stepwise $f(t)$ functions, the width of the steps being short with respect to the evolution time of the system.

Typical computed kinetic loops are shown in Fig. 11. For this numerical simulation, we have prepared the system at high temperature in the HS state (irrespective of the light intensity); then temperature was decreased with constant (negative) sweep rate, and increased with the same (i.e., opposite) rate. The typical kinetic features exhibited in the figure are discussed as follows.

(i) The widening of the entropy-driven hysteresis loop: note the bending of branches; detailed calculations show that the distortion is larger on the low-temperature side of the loop, in agreement with the asymmetrical behavior of the relaxation time, reported in Ref. 1.

(ii) The largest effects occur, of course, at low temperatures, because of the slowing down of the relaxation times of the metastable HS state. Again the distortion of the (LITH) hysteresis loop is asymmetrical, in agreement with the available experimental data.[5]

(iii) The low-temperature response of the system is tightly governed by the thermo-optical history of the sample. On the example given in Fig. 11, the closed loop results from a cooling down immediately followed by a warming up of the system. When starting from low temperatures, different curves are obtained according to the preparation of the system. When the process finishes at low temperature, the LITH loop may remain open as observed by the experimentalists.[5]

(iv) The maximum of n_{HS}, in the ascending branch results, schematically, from the competition between a constant excitation rate, and a relaxation rate which is progressively increased. It occurs at the vicinity of the light-induced temperature equilibrium.

We also investigated the kinetic distortion of the light-induced optical loops (LIOH). Figure 12 corresponds to an increase in intensity, followed by a decrease. As for the LITH effect, the calculated loop is open.

VII. COMPARISON TO EXPERIMENTS

We have reported in Figs. 13 and 14, typical experimental data for Fe^{II} spin transition solids (after Refs. 4,5): the HS

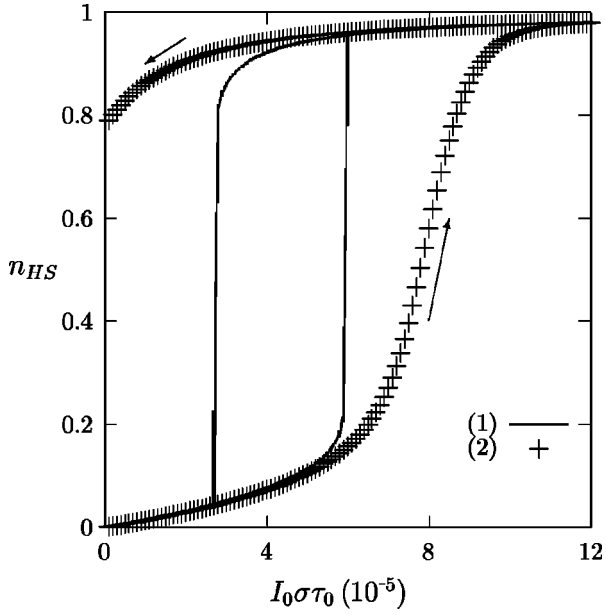

FIG. 12. A typical kinetic distortion of the optical hysteresis loop (crosses=2) with respect to the dynamic equilibrium curve (steady states, full line=1). The intensity sweep rate $\tau_0\sigma dI_0/dt = 5\times10^{-4}\ s^{-1}$. The parameters values are those of Figs. 1–8, with $T=70$ K.

fraction under continuous irradiation (550–600 nm) has been measured upon slow temperature variations, so as to obtain the LITH loops.

Obvious distortion from the ideal square shape can be analyzed, as a first approach, as due to the kinetic effects predicted in the previous section, despite of the long time usually devoted to such ''quasistatic'' experiments, typically

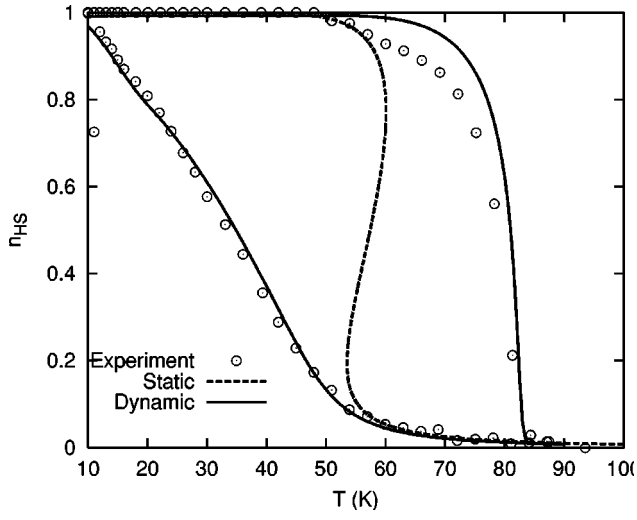

FIG. 13. Experimental data for the LITH loop of Fe($PM-BiA)_2(NCS)_2\cdots$ (Ref. 4). The n_{HS} values (HS fraction) have been derived from the magnetization data of Ref. 4, after zero-field splitting correction (see text). The solid line has been computed using Eq. (4.1) with the following parameter values: $I_0\sigma\tau_0(\times10^5)\simeq1.0$, $J=191$ K, $g=1408$, $\Delta=595$ K, and $E_a^0=1064$ K. The dotted line is the quasi-static curve (stationary solution, $dn_{HS}/dt=0$) computed using Eq. (4.9) with the same set of parameters.

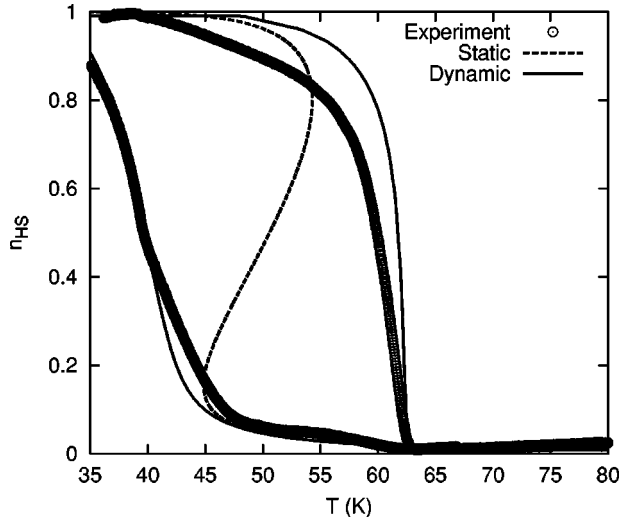

FIG. 14. Experimental data for the LITH loop of $Fe_{0.85}Co_{0.25}(btr)_2(NCS)_2\times H_2O$. The n_{HS} values (HS fraction) have been derived from optical reflectivity measurements (after Ref. 5. The solid line has been computed using Eq. (4.1) with the set of parameters $I_0\sigma\tau_0(\times10^5)\simeq1.0$, $J=171$ K, $g=4032$, $\Delta=518$ K, and $E_a^0=930$ K.

24 h or more for exploring the hole loop. The fits which are presented here as full lines account for the kinetic effects; the degeneracy parameter $\ln g_H/g_L=\Delta S/R$. The fitted parameters are: the intensity factor $I_0\sigma$ and the interaction parameter J; the thermal frequency factor $1/\tau_0$ and the activation energy E_a^0 values has been estimated from typical literature.[5] For illustrating the kinetic effects, we have computed the static curves, which we show as dotted lines.

In Fig. 13 magnetic data of Fe(PM-BiA)$_2$(NCS)$_2$ with $PM-BiA=N-(2$-Pyridylmethylene) aminobiphenyl,[4] have been corrected for a zero field splitting effect: the values obtained below 40 K on increasing temperature have been assigned to the saturate state of the system ($n_{HS}=1$), and consequently the n_{HS} values on decreasing temperatures in the same temperature range have been renormalized. The fitted values for the interaction parameter, $J=191$ K qualitatively agrees with the presence of a first-order entropy-driven transition at $T_{eq}\simeq170$ K with a hysteresis of 5 K: indeed the ratio $qJ/kT_{eq}=1.1$ is slightly larger than the threshold value 1 (see Sec. II).

In Fig. 14, the typical optical data of $Fe_{0.85}Co_{0.15}(btr)_2(NCS)_2\times H_2O$ (after Ref. 5) have been taken, in order to minimize the effect of bulk absorption of light.[4] This effect was minimized in the previous example by the recourse to a very thin sample. The fitted values of the interaction parameter, $J=171$ K, is consistent with the occurrence of a first-order transition at 110 K with a wide hysteresis loop (10 K): the ratio $qJ/kT_{eq}=1.55$ is in large excess of the threshold value 1. In this case, the kinetic effect in the cooling regime is particularly large, because of the slowing down of relaxation at low temperature. We discuss now the remaining discrepancies between the model and the experimental curves. An obvious effect of bulk absorption of light is to introduce an intensity distribution, such that the response of the system is the superimposition of LITH loops with light-induced equilibrium temperature actually spread over several K; with the larger effect on the low-temperature

side of the loop. Thus the asymmetrical distortion of the LITH loop can be explained.

It seems worth remarking that the agreement between model and experiments is surprisingly good for the LITH loops, in view of the discrepancies which have been observed for the sigmoidal relaxation curves (see Ref. 1, for example), and which have been attributed to the onset of correlations. A tentative explanation might lie in the random effect of light, which continuously tends to destroy the correlations.[41]

VIII. CONCLUSION

We have investigated the effect of a permanent photoexcitation on spin transition systems. The excitation has been accounted for by introducing an adapted rate transition in the detailed balance equation. The resulting master equation, which governs the dynamics of the system, has been established and expressed in terms of the average high-spin fraction. The state equation of the steady states (dynamic equilibrium) has been derived and leads to instabilities, as a function of temperature, intensity and pressure. The corresponding hysteresis loops are denoted LITH (thermal), LIOH (optical), and LIPH (pressure).

The phase diagram of the system has been determined analytically, i.e., the conditions for the light-induced loops to occur have been expressed. The possible collapse between the low-temperature (light-induced) and high-temperature (entropy-driven) instabilities has been considered and results in open hysteresis loops at finite temperatures.

The effects of the measurement time, i.e., the kinetic distortions with respect to the steady states properties, have been determined by numerical resolution of the master equation; the computed curves qualitatively agree with the few available experimental data. Further work, treating the master equation beyond the mean-field approximation, is in progress, aiming at establishing the role of correlations[42] and dilution in the system.

ACKNOWLEDGMENTS

The authors would like to thank Dr. J. Hodges for reading the manuscript, Professor J. Linarès, Dr. J. F. Létard, and Mr. A. Goujon for communicating their experimental data. LMOV is supported by CNRS, as ''Unité Mixte de Recherche'' (UMR Grant No. 8634). The CEE financial support (TMR action TOSS, Contract No. CT98-0199) is acknowledged.

*Email address: kbo@physique.uvsq.fr

[1] K. Boukheddaden, I. Shteto, B. Hôo, and F. Varret, preceding paper, Phys. Rev. B **62**, 14 796 (2000).

[2] P. Gütlich, Struct. Bonding (Berlin) **44**, 83 (1981); E. König, *ibid.* **76**, 51 (1991); O. Kahn, Curr. Opin. Solid State Mater. Sci. **1**, 547 (1996).

[3] A. Hauser, Coord. Chem. Rev. **11**, 275 (1991); P. Gütlich, A. Hauser, H. Spiering, Angnew Chem. Int. Ed. Engl. **33**, 2024 (1994); A. Hauser, Comments Inorg. Chem. **17**, 17 (1995); R. Hinek, H. Spiering, P. Gütlich, and A. Hauser, Chem.-Eur. J. **2**, 1435 (1996).

[4] J. F. Létard, P. Guinneau, L. Rabardel, J. A. K. Howard, A. E. Goeta, D. Chasseau, and O. Kahn, Inorg. Chem. **37**, 4432 (1998); Chem. Eur. J. **2**, 1435 (1996).

[5] A. Desaix, O. Roubeau, J. Jeftic, J. G. Haasnoot, K. Boukheddaden, E. Codjovi, J. Linarés, M. Nogués, and F. Varret, Eur. Phys. J. B **6**, 183 (1998).

[6] S. Decurtins, P. Gütlich, C. P. Köhler, H. Spiering, and A. Hauser, Chem. Phys. Lett. **1**, 139 (1984); S. Decurtins, P. Gütlich, K. M. Hasselbach, A. Hauser, and H. Spiering, Inorg. Chem. **24**, 2174 (1985).

[7] P. Adler, H. Spiering and P. Gütlich, J. Phys. Chem. Solids **50**, 587 (1989).

[8] A. Bousseksou, C. Place, J. Linares, and F. Varret, J. Magn. Magn. Mater. **104**, 225 (1992).

[9] J. J. McGarvey and I. Lauthers, J. Chem. Soc. Chem. Commun. **1982**, 906.

[10] F. Varret, K. Boukheddaden, J. Jeftic, and O. Roubeau, Mol. Cryst. Liq. Cryst. **335**, 561 (1999).

[11] H. Spiering, T. Kohlhaas, H. Romstedt, A. Hauser, C. Bruns-Yilmaz, J. Kusz, and P. Gütlich, Coord. Chem. Rev. **190-192**, 629 (1999).

[12] J. Wajnflasz, J. Phys. Status Solidi **40**, 537 (1970).

[13] J. Wajnflasz and R. Pick, J. Phys. (Paris), Colloq. **32**, C1 (1971).

[14] R. J. Glauber, J. Math. Phys. **4**, 294 (1963).

[15] J. D. Gunton and M. Droz, in *Introduction to the Theory of Metastable and Unstable States*, Vol. 183 of Lecture Notes in Physics (Springer-Verlag, Berlin, 1983).

[16] M. Suzuki and R. Kubo, J. Phys. Soc. Jpn. **24**, 51 (1968); Y. Saito, R. Kubo, J. Stat. Phys. **15**, 233 (1976).

[17] H. Spiering, E. Meissner, H. Köpen, E. W. Müller, and P. Gütlich, Chem. Phys. **68**, 65 (1982); A. Hauser, P. Gütlich, and H. Spiering, Inorg. Chem. **25**, 4345 (1986).

[18] A. Hauser, J. Jeftic, H. Romstedt, R. Hinek, and H. Spiering, Coord. Chem. Rev. **190-192**, 471 (1999).

[19] A. Hauser, J. Chem. Phys. **94**, 2741 (1991).

[20] M. Hasegawa, Y. Suzuki, F. Suzuki, and H. Nakanishi, J. Polym. Sci., Polym. Chem. Ed. **7**, 743 (1969); Y. Sasada, H. Shimanouchi, H. Nakanishi, and M. Hasegawa, Bull. Chem. Soc. Jpn. **44**, 262 (1971); J. D. Dunitz, Pure Appl. Chem. **63**, 177 (1963); N. M. Peachey and C. J. Eckhardt, J. Phys. Chem. **97**, 10 849 (1993); T. Luty and C. J. Eckhardt, J. Am. Chem. Soc. **117**, 2441 (1995). .

[21] E. Salomons, P. Bellon, F. Soisson, and G. Martin, Phys. Rev. B **45**, 4582 (1992); F. Soisson, P. Bellon, and G. Martin, *ibid.* **46**, 11 332 (1992).

[22] M. H. Lemée-Cailleau, M. Le Cointe, H. Cailleau, T. Luty, F. Moussa, J. Roos, D. Brinkmann, B. Toudic, C. Ayache, and N. Karl, Phys. Rev. Lett. **79**, 1690 (1997); S. Koshihara, Y. Takahashi, H. Sakai, Y. Tokura, and T. Luty, J. Phys. Chem. **103**, 2592 (1999).

[23] *Optical Properties of Low-Dimensional Metals*, edited by T. Ogawa and Y. Kanemitsu (World Scientific, Singapore, 1995).

[24] N. Nagaosa and T. Ogawa, Phys. Rev. B **39**, 4472 (1989); in *Relaxation of Excited States and Photo-Induced Structural Phase Transitions*, edited by K. Nasu, Springer Series in Solid-State Science No. 124 (Springer, Berlin, 1997).

[25] K. Koshino and T. Ogawa, J. Phys. Soc. Jpn. **67**, 2174 (1998).

[26] K. Iwano, Phys. Rev. B **61**, 279 (2000).

[27] Y. Ogawa, A. Mino, S. Koshihara, K. Koshino, T. Ogawa, C.

Urano, and H. Takagi, Phys. Rev. Lett. **84**, 3181 (2000).
[28] T. Tome and M. J. de Oliveira, Phys. Rev. A **40**, 6643 (1989).
[29] N.G. Van Kampen, *Stochastic Processes in Physics and Chemistry* (North-Holland, Amsterdam, 1992).
[30] J. T. Ubbink, Physica (Amsterdam) **52**, 253 (1971).
[31] M. Mishino, Y. Yamaguchi, and S. Miyashita, Phys. Rev. B **58**, 1 (1998).
[32] F. Varret, H. Constant-Machado, J. L. Dormann, A. Goujonj, J. Jeftic, M. Nogués, A. Bousseksou, S. Klokishner, A. Dolbecq, and M. Verdaguer, Hyperfine Interact. **113**, 37 (1998).
[33] O. Sato, T. Iyoda, A. Fujishima, and K. Hashimoto, Science **272**, 704 (1996).
[34] A. Goujon, O. Roubeau, F. Varret, A. Dolbecq, A. Bleuzen, and M. Verdaguer, Eur. Phys. J. B **14**, 115 (2000).
[35] R. Kopelman, Science **241**, 1620 (1988).
[36] H. Tomita and S. Miyashita, Phys. Rev. B **46**, 8886 (1992).
[37] I. Prigogine, R. Lefever, J. S. Turner, and J. W. Turner, Phys. Lett. **35**, 1453 (1975); in *Nonequilibrium Systems. From Dissipative Structure to Order Through Fluctuations* (Wiley-Interscience Publication, New York, 1988), p. 339; in *Symmetries and Broken Symmetries in Condensed Matter Physics*, edited by N. Boccara (IDSET, Paris, 1981); S. Chandrasekhar, *Hydrodynamic Stability* (Oxford, Clarendon, 1961).
[38] R. Brout, in *Phase Transitions* (Benjamin, New York, 1965).
[39] N. Menendez, E. Codjovi, K. Boukheddaden, and F. Varret (unpublished).
[40] O. Roubeau, J. G. Haasnoot, J. Linares, and F. Varret, Liq. Cryst. **335**, 583 (1999).
[41] H. Romstedt, A. Hauser, and H. Spiering, J. Phys. Chem. Solids **52**, 265 (1997).
[42] B. Hôo, K. Boukheddaden, and F. Varret, Eur. Phys. J. B **17**, 449 (2000).